STIMULUS REPORT

blood advances

CRISPR genome editing of murine hematopoietic stem cells to create *Npm1-Alk* causes ALK$^+$ lymphoma after transplantation

Soumya Sundara Rajan,[1,2] Lingxiao Li,[2,3] Mercedes F. Kweh,[2,3] Kranthi Kunkalla,[2,4] Amit Dipak Amin,[2,3] Nitin K. Agarwal,[2,4] Francisco Vega,[2,4] and Jonathan H. Schatz[2,3]

[1]Sheila and David Fuente Graduate Program in Cancer Biology, [2]Sylvester Comprehensive Cancer Center, [3]Division of Hematology, Department of Medicine, and [4]Division of Hematopathology, Department of Pathology and Laboratory Medicine, University of Miami Miller School of Medicine, Miami, FL

Key Points

- CRISPR/Cas9 genomic editing of wild-type hematopoietic stem cells generates *Npm1-Alk*, leading to ALK$^+$ large-cell lymphomas in recipients.
- CD30$^+$ postthymic T-cell lymphomas are polyclonal but transplantable to secondary recipients with long latency.

Introduction

Fusion oncogenes from recurrent chromosomal rearrangements drive many hematologic malignancies.[1] Traditional modeling of these lesions in mice involves retroviral introduction of human fusion oncogenes to murine hematopoietic progenitors and subsequent syngeneic transplantation. Alternatively, the oncogenes can be engineered into the germline under lineage-specific promoters. For example, introduction of *BCR-ABL*,[2,3] derived from chronic myeloid leukemia (CML), to progenitors causes a fatal myeloproliferative disease similar to accelerated-phase CML but does not capture the prolonged chronic phase of human CML.[4] *NPM1-ALK*, derived from anaplastic lymphoma kinase (ALK)$^+$ anaplastic large-cell lymphoma (ALCL) is another classic fusion that drove breakthrough animal modeling for T-cell lymphomas.[5] First described in 1985, ALK$^+$ ALCL is a T-cell non-Hodgkin lymphoma constituting ~2% of lymphoma diagnoses overall; it is seen most commonly in adolescents and young adults.[6] It is the most frequent pediatric mature T-cell malignancy. Pathologically, ALK$^+$ ALCL cells have an irregular blastic morphology, including large nuclei and scant cytoplasm. The disease is diagnosed by expression of the characteristic ALK protein and CD30, but T-cell surface markers are variably lost, leaving many cases with a null-cell phenotype.[7-9] Previous use of *NPM1-ALK* in murine lymphoma models demonstrated the gene's potent transforming properties but did not fully recapitulate the phenotype of human ALK$^+$ ALCL. Retroviral infection of bone marrow progenitor cells with *NPM1-ALK* led to B-cell lymphomas after transplantation to recipients.[10] Transgenic engineering of *NPM1-ALK* into the murine genome under Vav or CD2 promoters also resulted in B lymphomas.[11,12] Chiarle et al achieved a T-cell phenotype by placing *NPM1-ALK* under a CD4 promoter, but animals developed immature T-cell lymphomas more similar to lymphoblastic lymphoma, and leaky expression drove B-lineage plasma-cell neoplasms in about a third.[13] CRISPR/Cas9 genome editing recently resulted in breakthrough modeling of ALK$^+$ lung cancer through generation of *Eml4-Alk*, homologous to the human fusion oncogene, through introduction of genomic breakpoints.[14] Here, we successfully adapted these techniques to modeling hematologic malignancy for the first time by generating *Npm1-Alk* in the genome of transplantable hematopoietic stem cells (HSCs).

Methods

Additional detailed information is provided in supplemental Methods.

Cell culture

HSCs were isolated from fetal livers at embryonic day 14.5 and grown in RPMI 1640 supplemented with 10% fetal bovine serum, 10% WEHI supernatant, interleukin-3 (IL-3) (10 μg/mL), IL-6 (10 μg/mL), and stem cell factor (10 μg/mL). To prevent differentiation, HSCs were maintained in culture for <72 hours. Splenocytes were cultured in RPMI 1640 supplemented with 20% fetal bovine serum.

Submitted 24 August 2018; accepted 6 May 2019. DOI 10.1182/bloodadvances.2018025247.

The full-text version of this article contains a data supplement.

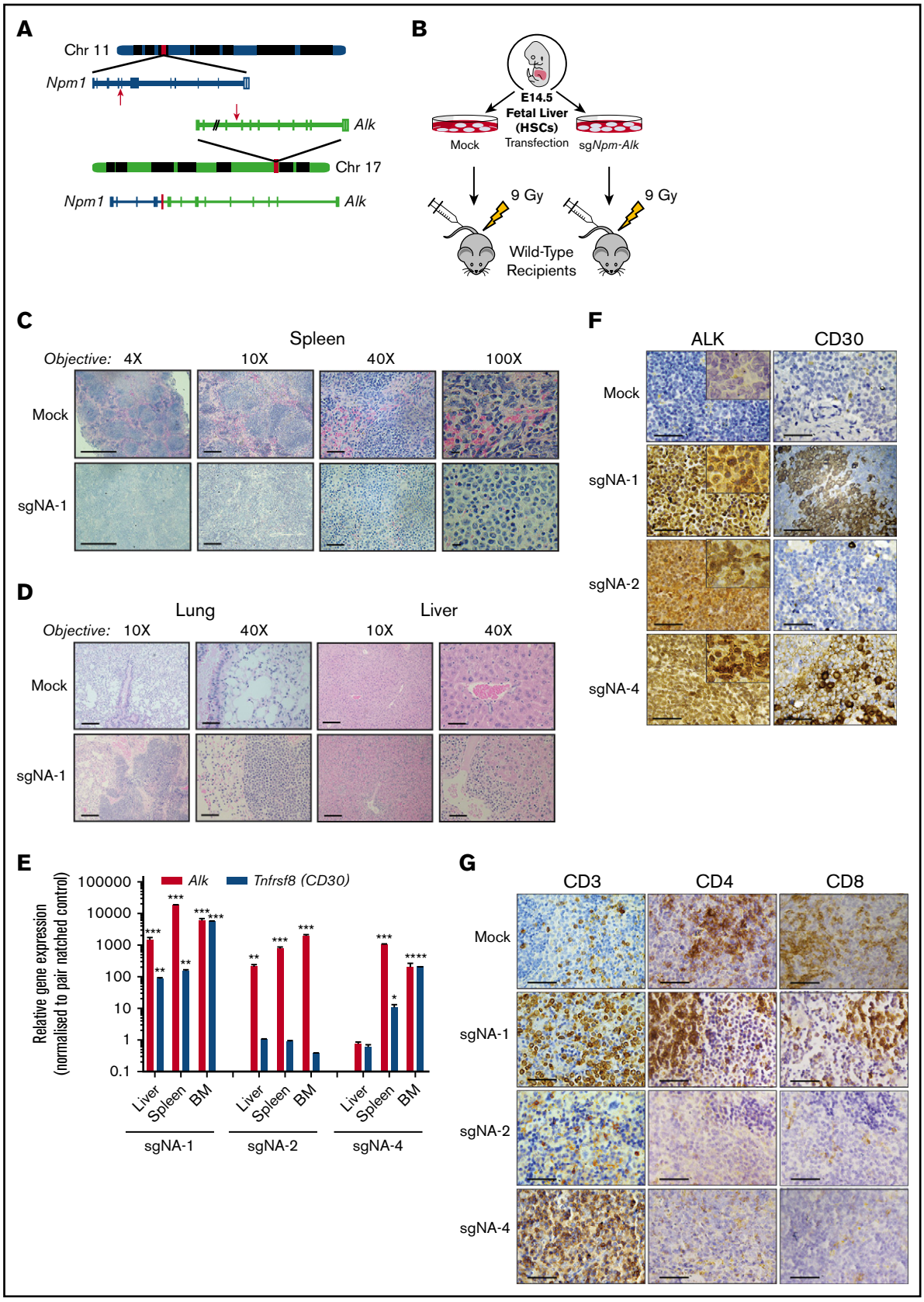

Figure 1. ALK$^+$ lymphomas develop after transplantation of HSCs transfected with a CRISPR vector targeting breakpoints to *Npm1* and *Alk* (sgNA). (A) Breakpoints (red arrows) in the mouse chromosome leading to creation of t(11:17) involving *Npm1* and *Alk* and the predicted *Npm1-Alk* fusion gene. (B) Experimental design

HSC modification and transplantation

Individual fetal livers from wild-type C57BL/6 mice with 2×10^5 HSCs each were divided to undergo CRISPR vs mock transfection (Figure 1B). We used Lipofectamine 3000 transfection reagent, with or without 3 μg pX330, with single guide RNAs targeting *Npm1* and *Alk* (sgNA; Figure 1A)[14] over 2 days. After overnight incubation in fresh media, transfected HSCs were injected via the tail vein into sublethally irradiated (4.5 G × 2, separated by 2 hours) syngeneic wild-type C57BL/6 recipients. All primary recipients were 9 weeks old at the time of transplantation. For secondary recipients, 10^6 splenocytes from the primary recipients were transplanted into irradiated wild-type C57BL/6 mice via the tail vein. These mice were also 9 weeks old at the time of transplantation.

Histology and immunohistochemistry

Formalin-fixed paraffin-embedded tissue sections, produced per standard protocols, were used to make H&E-stained and immunohistochemistry (IHC) pathology slides. Primary IHC antibodies were anti-ALK (Abcam, ab180607), anti-CD30 (Invitrogen, MA512532), anti-CD3 (Abcam, ab16669), anti-CD4 (Invitrogen, 14-9766-82), and anti-CD8a (Invitrogen, 14-0195-80). After secondary antibody and counterstaining, all slides were subject to expert hematopathology review (F.V.).

Fluorescence-activated cell sorting analysis

Splenocytes were collected, passaged transiently in vitro, and stained with the following antibodies: B220 (BD Bioscience, 552772), IgM (BD Bioscience, 553437), and Thy1.2 (eBioscience, 12-0902-82). Viable cells were gated through phycoerythrin staining, and stained samples were run on the Attune NxT analyzer. Data were then analyzed using FlowJo software (TreeStar, Inc.).

Clonality analysis

Amplification and sequencing of (TCRB/IGH/IGKL/TCRAD/TCRG) CDR3 were performed with immunoSEQ (Adaptive Biotechnologies, Seattle, WA). The clonal repertoire is determined using the Shannon entropy-based clonality index, which ranges from 0 to 1, with index values < 0.5 being polyclonal.[13,]

Results and discussion

The *Npm1* and *Alk* genes on murine chromosomes 11 and 17, respectively, contain intronic breakpoints that can create an in-frame fusion *Npm1-Alk* oncogene closely analogous to human *NPM1-ALK* (Figure 1A; supplemental Figure 1A).[14] We transfected 3T3 cells with sgNA vector encoding Cas9 and single guide RNAs targeting these breakpoints and confirmed generation of *Npm1-Alk* (supplemental Figure 1B-C), including sequence confirmation of an expected 1.5-kb *Npm1-Alk* PCR band (supplemental Figure 1D). CRISPR-generated *Npm1-Alk* transforms IL-3–dependent Ba/F3 cells[15,16] but has not previously been compared with human *NPM1-ALK*. We infected the cytokine-dependent murine pro-B cell line FL5.12 with vector, *Npm1-Alk*, or *NPM1-ALK* with GFP coexpression and cycled them through IL-3 withdrawal and rescue, resulting in *Npm1-Alk* enrichment similar to *NPM1-ALK* (supplemental Figure 1E). Both the human and mouse alleles transformed the FL5.12 cells to proliferation in cytokine-free media. *Npm1-Alk*–transformed cells are highly sensitive to clinical ALK kinase inhibitors (supplemental Figure 1F-G), but differences in the ALK kinase domains resulted in differential sensitivity patterns, including relative crizotinib and ceritinib sensitivity but alectinib resistance.

We next divided C57BL/6 murine HSCs from a single fetal liver for mock vs sgNA transfection and confirmed detection of *Npm1-Alk* in the sgNA-transfected cells (supplemental Figure 2A-B), including Sanger sequencing confirmation of the fusion gene from the polymerase chain reaction (PCR) product (data not shown; same result as supplemental Figure 1D). We repeated paired sgNA/mock transfections of HSCs isolated from individual fetal livers and transplanted them into wild-type C57BL/6 recipients subjected to sublethal irradiation (Figure 1B). No recipients died during the initial 3-4 weeks following transplantation, indicating successful engraftment of transplanted HSCs. All were unremarkable until posttransplant day 270, when an animal transplanted with sgNA-modified HSCs (sgNA-1) became moribund and was euthanized in parallel with its paired mock control. Pathologic analysis showed that, although the mouse transplanted with mock-transfected HSCs was phenotypically normal, the mouse transplanted with CRISPR-transfected HSCs had lymphoma completely effacing the normal architecture of the spleen (Figure 1C). In addition, lymphoma cells invaded multiple organs of the CRISPR-modified HSC recipient, including lung, liver (Figure 1D), and kidney (data not shown). Thereafter, the remaining mice were euthanized, revealing lymphoma in 3 of 4 mice (overall) transplanted with sgNA-modified HSCs (supplemental Figure 2C-D). Like sgNA-1, mouse sgNA-2 had lymphoma involvement of nonhematologic organs (lung and liver, supplemental Figure 2D), whereas disease in mouse sgNA-4 was confined morphologically to the spleen. An additional mouse transplanted with CRISPR-transfected HSCs (sgNA-3) never became moribund and was phenotypically normal when sacrificed a year after transplantation (data not shown). All of the mock-transfected paired control animals were phenotypically normal (Figure 1C-D; others not shown). Fluorescence-activated cell sorting analysis of splenocytes from diseased and control animals showed an increased presence of T-lineage lymphocytes based on Thy1.2 cell surface expression in animals sgNA-1 and sgNA-4,

Figure 1. (continued) for transplantation of transfected wild-type HSCs to sublethally irradiated primary recipients. (C) Photomicrographs of spleen (40×, 100×, 400×, and 1000× magnification) from the initially moribund animal, sgNA-1, transplanted with CRISPR-transfected HSCs and from the paired control animal transplanted with mock-transfected HSCs from the same fetal liver (hematoxylin and eosin [H&E] stain). (D) Photomicrographs of lung and liver (100× and 400× magnification) from the same animals as in panel C, showing invasion of lymphoma into these organs (H&E stain). (E) *Alk* kinase domain and *Tnfrsf8* (CD30) expression by TaqMan qRT-PCR in primary recipients of sgNA-transfected HSCs normalized to paired mock controls. RNA was freshly isolated from the indicated tissues. Data are mean ± standard error of the mean of 3 technical replicates. (F) IHC staining of large-cell lymphomas in spleens compared with spleen from a mock-control animal for ALK and CD30 taken under at 600× magnification; 1000× magnification insets are shown for ALK. For full-size 1000× micrographs, see supplemental Figure 2F. (G) IHC staining for common T-cell surface markers in mock-treated spleen compared with large-cell lymphomas. Photomicrographs were taken under at 600× magnification. For low-power (40×) and high-power (1000×) views, see supplemental Figure 4. Scale bars, 1 mm (40×), 200 μm (100×), 50 μm (400×), 50 μm (600×), 10 μm (1000×). $^*P < .01$, $^{**}P < .001$, $^{***}P < .0001$, 2-tailed Student *t* test. BM, bone marrow.

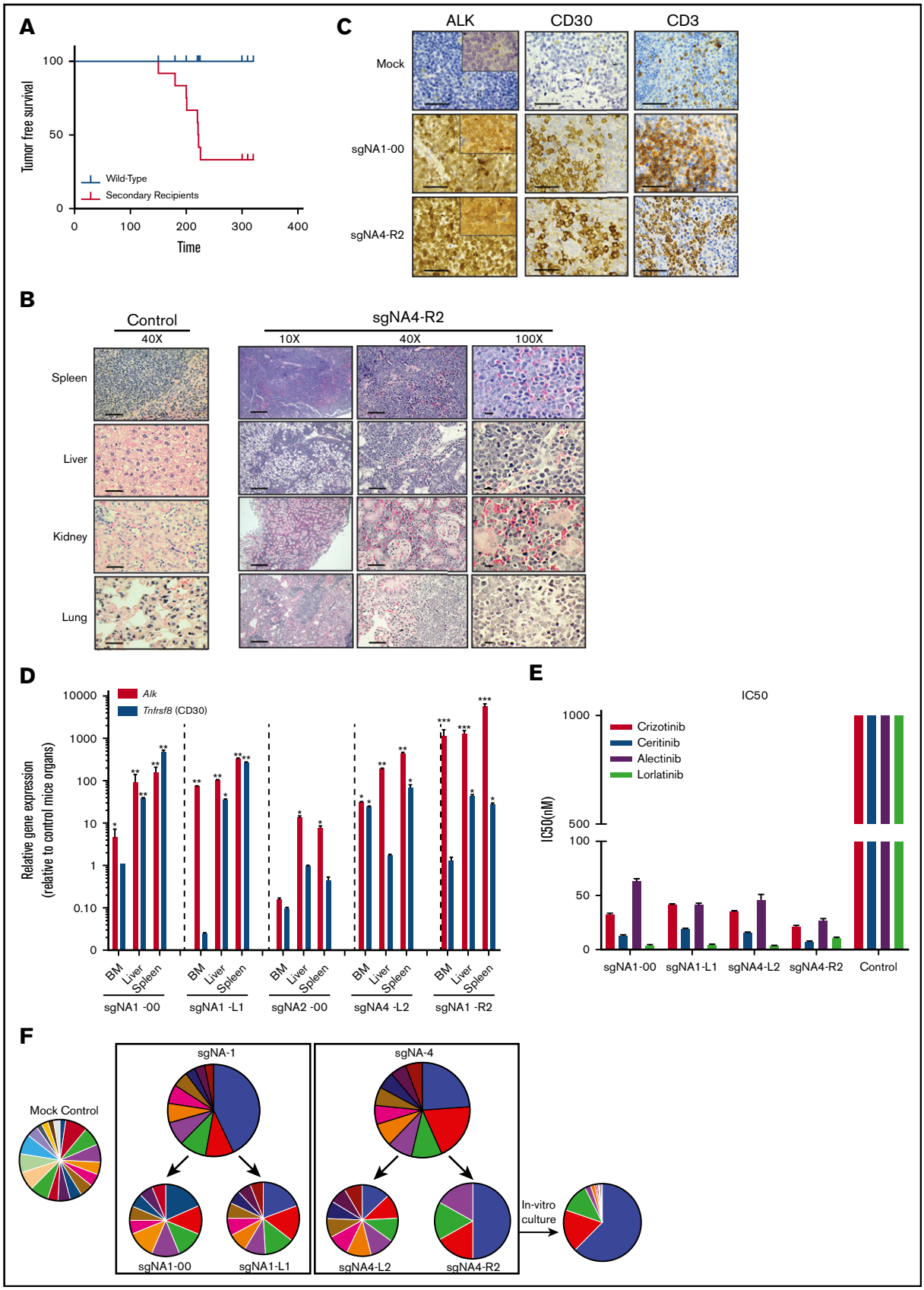

Figure 2.

whereas sgNA-2 had decreased numbers of T cells (supplemental Figure 2E). This mouse instead had a prominent population of $B220^+$ IgM^- cells, consistent with a B-cell lymphoma phenotype in this animal. We next assessed expression of ALK and CD30, pathologic hallmarks of human ALK^+ ALCL. Quantitative reverse-transcription PCR (qRT-PCR) was used to assess expression of the murine *Alk* kinase domain in diseased recipients, normalized to corresponding tissues from each animal's paired mock control. The lymphoma-bearing animals had 10× to 10 000× expression in bone marrow, spleen, and other affected organs (Figure 1E). Expression of *Tnfrsf8*, which encodes murine CD30, was similarly elevated in sgNA-1 and sgNA-4 but not in sgNA-2. Therefore, we carried out IHC evaluation for these markers, which showed, consistent with the quantitative PCR (qPCR) results, high ALK protein in the spleens of all of the diseased animals, including the nuclear staining pattern that is distinctive of human NPM1-ALK (Figure 1F; micrographs taken with 60× objective, 100× objective insets for ALK; full-size 100× micrographs are provided as supplemental Figure 2F).[17,18] sgNA-1 and sgNA-4 showed strong cell surface staining for CD30, whereas sgNA-2, like human ALK^+ large B-cell lymphoma, was $CD30^-$.[19,20] We used reverse-transcription PCR primers spanning the *Npm1-Alk* fusion to confirm its detection in tumor-affected tissues from transplanted mice (supplemental Figure 3A). Generation of *Npm1-Alk* in HSCs leads to ALK^+ lymphomas in transplant recipients after a long latency.

We further characterized the surface phenotype of these lymphomas, focusing on the T-cell markers CD3, CD4, and CD8, which are highly variable in human ALK^+ ALCL; they are commonly absent, leading to a null-cell phenotype that requires T-cell receptor (TCR) clonality studies to confirm T-cell origin.[21,22] Both animals with suspected T-cell lymphomas, sgNA-1 and sgNA-4, had scattered positivity for CD3, and sgNA-1 also had patches in the spleen that were strongly positive for CD4 and CD8 (Figure 1G; high- and low-magnification views in supplemental Figure 4). sgNA-4 was negative for CD4 and CD8, whereas sgNA-2 was negative for all 3 T-cell markers, as expected. To further clarify the disease phenotype of sgNA-1, we assessed CD4 and CD8 in tumors invasive to other organs, which occurred in this animal but not in sgNA-4. The perivascular lymphomas that arose in the lung of this animal were strongly $CD4^+$ and $CD8^+$ (supplemental Figure 3B, see "Discussion"). In sum, pathologic analyses show variations in morphology and cell surface markers, potentially consistent with multiple lymphomas, having arisen simultaneously, which could be assessed through TCR clonality studies.

We next tested transplantability of primary tumors to secondary recipients through tail vein injection of 10^6 splenocytes from primary recipients to wild-type mice after 4-Gy irradiation. Available cell numbers permitted 12 secondary transplantations, 5 each from sgNA-1 and sgNA-4 (T-cell lymphomas) and 2 from sgNA-2 (B cell). Disease onset in all secondary recipients is grouped in Figure 2A, showing lymphomas in 9 of 12 mice beginning by day 180. When the first mouse became moribund, we analyzed peripheral blood from all secondary recipients for expression of *Alk* and *Tnfrsf8* using qPCR (supplemental Figure 5A). Seven of 8 animals that had elevated ALK expression at this time point subsequently developed disease (red boxes). Pathologic assessment showed lymphomas similar to primary recipients infiltrating spleen and other organs (Figure 2B, and data not shown), including 1 mouse with nodal lymphoma (supplemental Figure 5B). Affected animals had enlarged livers and spleens compared with controls sacrificed in parallel (supplemental Figure 5C). Tumors in T-lymphoma recipients showed ALK, CD30, and CD3 IHC staining similar to primary recipients (Figure 2C; supplemental Figure 3C). Diseased secondary recipients transplanted with T lymphomas, like primary recipients, had overexpression of *Alk* and *Tnfrsf8*, whereas only *Alk* was elevated in a diseased secondary recipient of tumor cells from sgNA-2 (Figure 2D). *Npm1-Alk* was confirmed by reverse-transcription PCR in transplanted mice (supplemental Figure 5D). Protein expression of ALK and its established downstream effectors were also seen in transplanted mice but not wild-type splenocytes via western blotting performed on unselected splenocytes (supplemental Figure 5E). These cells had undergone cryopreservation before this analysis was performed and showed a banding pattern in response to a murine-specific ALK antibody, consistent with partial degradation of NPM1-ALK, as reported previously for the human protein.[23] A high-molecular-weight ALK band also was detected, consistent with perinuclear aggregate NPM1-ALK, which is well described.[24,25] The wild-type control splenocytes did not show any reactivity to the murine ALK antibody. Tumor cells from spleens isolated from sgNA4-R2, sgNA1-00, sgNA1-L1, and sgNA4-L2 proliferated transiently and were highly sensitive to ALK inhibitors, with the sensitivity pattern mirroring *Npm1-Alk*–transformed FL5.12 cells (Figure 2E; supplemental Figure 5F).

We next assessed TCR clonality of the primary recipients that developed T-cell lymphomas and 2 secondary recipients transplanted with tumor cells from each of these primaries using GeneScan.[26,27] The diversity of β-chain rearrangements is plotted as pie charts (Figure 2F; supplemental Figure 5G). Primary recipients were

Figure 2. *Npm1-Alk*$^+$ lymphomas are transplantable, polyclonal, and highly sensitive to ALK kinase inhibitors. (A) Lymphoma onset in secondary recipients with wild-type C57/BL6 mice as control. (B) Micrographs of representative H&E histology of the indicated organs from a secondary recipient of T-cell lymphoma compared with wild-type control (100×, 400×, and 1000× magnification). (C) Micrographs of IHC staining of spleens of secondary recipients for ALK, CD30, and CD3 with a wild-type control as comparison (600× magnification; ALK insets at 1000×). (D) *Alk* and *Tnfrsf8* (CD30) expression by TaqMan qRT-PCR in the indicated tissues freshly isolated from 5 representative secondary recipients. Data are mean ± standard error of the mean from 3 technical replicates. (E) IC_{50} (50% inhibitory concentration) values calculated from viability curves of lymphoma cells exposed to the indicated clinical ALK-specific tyrosine kinase inhibitors. Lymphoma cells from the indicated animals proliferated transiently in tissue culture. The murine T-cell line MOHITO was used as control. (F) TCR β-chain diversity plotted as pie charts for splenocytes, with each color representing a unique TCR clone in the sequencing data, from a representative mock control animal and the 2 animals that developed T-cell lymphomas (sgNA-1 and sgNA-4) plus 2 secondary recipients from each primary recipient compared with mock control mouse. We also rechecked the diversity of the cells from 1 secondary recipient, as indicated, after 12 days of culture in vitro. Clonality was determined using the Shannon's entropy-based clonality index. This value ranges from 0 to 1, in which values approaching 1 indicate a monoclonal population. The cutoff for determining polyclonality was 0.5 (see also supplemental Figure 3G). Scale bars, 200 μm (100×), 50 μm (400×), 50 μm (600×), 10 μm (1000×). $^*P < .01$, $^{**}P < .001$, $^{***}P < .0001$, 2-tailed Student *t* test.

polyclonal but had significantly decreased clonal diversity compared with mock controls. Additionally, clones identical to the primary recipients were found when the analysis was performed on splenocytes from diseased secondary recipients. Therefore, these lymphomas derive from postthymic T cells but were not monoclonal, consistent with multiple separate transformations having occurred during disease latency in T cells containing the *Npm1-Alk* translocation.

In sum, we demonstrate transplantable ALK-driven lymphomas resulting from creation of *Npm1-Alk* by CRISPR genome editing of murine HSCs. The long latency is consistent with natural progression to disease onset after introduction of a single genetic lesion formed from endogenous murine loci. *Npm1-Alk*$^+$ transplanted HSCs could only have contained 1 copy of the fusion because *Npm1* is an essential gene, and its other copy must remain intact.[18,28] Therefore, these cells accurately represent the initiating genotype of human ALK$^+$ ALCL and resulted in a phenotype with similarities to and differences from human disease. Specifically, T-cell lymphomas had a large-cell morphology, had strong expression of cell surface CD30, and showed TCR rearrangements indicating progression through key steps of thymic maturation. Tumors were oligoclonal compared with mock controls but not monoclonal like human ALCL. Different clones that arose appeared to have various cell surface phenotypes, with differential expression of CD3, CD4, and CD8 among tumor cells, including within the same diseased spleen, illustrated especially by the primary recipient sgNA-1. Tumors invading other organs in this animal were CD4$^+$ CD8$^+$, a phenotype that is rarely seen in human ALK ALCL, in which expression of CD4 alone or neither marker are most common.[9,29] Animals did not develop a primarily nodal lymphoma as is seen in most human patients; instead, disease involved the spleen, with variable spread to liver, lung, and kidney.

Regardless, the proof-of-principle established here is widely adaptable to additional hematologic malignancies and may help to generate preclinical models with increased fidelity. Piganeau et al used a transcription activator-like effector nuclease approach to generate t(2;5)(p23;q35)/*NPM1-ALK* in cultured human cells through generation of double-stranded DNA breaks, but this approach was not used to model the disease.[30] Utility of our model in preclinical studies is limited by long disease latency in secondary recipients (minimum 180 days) and the phenotypic variability outlined above. Serial passaging of these tumors through additional recipients may or may not reveal isolated clones that result in tumor phenotypes with high fidelity for human ALK$^+$ ALCL to fuel preclinical treatment experiments. Tumor cells from primary and secondary recipients proliferated transiently in vitro in media not supplemented with cytokines, but they did not become long-term cell lines. This also could change after passages through additional recipients moving forward or with the use of T-cell stimulatory cytokines.

Early animal-modeling efforts with *NPM1-ALK* (discussed in "Introduction") left the cell of origin for ALK$^+$ ALCL unclear, and it still has not been definitively revealed. Recently, Malcolm et al shed key light on this question, showing that *NPM1-ALK*$^+$ thymic precursors use the fusion oncogene to bypass the β-selection checkpoint before moving to the periphery to establish systemic lymphomas.[31] By engineering the endogenous translocation into a subset of HSCs, our approach may have allowed recapitulation of this process, as opposed to earlier transgenic approaches placing *NPM1-ALK* expression under the control of specific T-lineage promoters. Additional evidence also exists for *NPM1-ALK* arising in early stem or progenitor cells. Trümper et al showed in 1998 that 14 of 29 healthy individuals (48%) had *NPM1-ALK* detectable by high-sensitivity PCR in peripheral blood,[32] and even umbilical cord blood from healthy newborns showed evidence of the fusion in ~2%[33] (although this was not linked to later onset of ALK$^+$ ALCL in either study). The polyclonal phenotype that we observed is consistent with multiple individual clones having undergone transformation separately in the mice that developed T lymphomas. Therefore, these primary diseases were molecularly more heterogeneous than human ALK$^+$ ALCL.

Acknowledgments

The authors thank the Sheila and David Fuente Graduate Program in Cancer Biology at the University of Miami and are extremely grateful to Andrea Ventura (Memorial Sloan Kettering Cancer Center, New York, NY) and Danilo Maddalo (Novartis) for providing the sg*Npm-Alk* plasmid. The authors thank Mingjiang Xu (University of Miami) for developing the pathology core and helping with the slides for H&E staining and IHC, and as well as the laboratory of Feng-Chun Yang (University of Miami) for extensive use of the microscope camera.

This work was supported by National Institutes of Health, National Cancer Institute grant 1R01CA190696-01 (J.H.S.).

S.S.R. was a PhD candidate at the University of Miami, and this work is submitted in partial fulfillment of the requirement for a PhD.

Authorship

Contribution: S.S.R. and A.D.A. performed qPCR and clonality analysis; L.L. transplanted mice and performed fluorescence-activated cell sorting and IHC; S.S.R., M.F.K., K.K., and N.K.A. performed IHC staining and analyzed the results; F.V. analyzed the IHC and pathology slides; S.S.R. and J.H.S. designed the experiments, analyzed the results, and wrote the manuscript; and J.H.S. provided funding for this study.

Conflict-of-interest disclosure: The authors declare no competing financial interests.

ORCID profiles: F.V., 0000-0001-5956-452X; J.H.S., 0000-0003-1842-228X.

Correspondence: Jonathan H. Schatz, Batchelor Children's Research Institute, University of Miami, 1580 NW 10th Ave, Room 419, Miami, FL 33137; e-mail: jschatz@med.miami.edu.

References

1. Nelson KN, Peiris MN, Meyer AN, Siari A, Donoghue DJ. Receptor tyrosine kinases: translocation partners in hematopoietic disorders. *Trends Mol Med*. 2017;23(1):59-79.

2. Nowell PC, Hungerford DA. Chromosome studies on normal and leukemic human leukocytes. *J Natl Cancer Inst*. 1960;25(1):85-109.

3. Hochhaus A, Larson RA, Guilhot F, et al; IRIS Investigators. Long-term outcomes of imatinib treatment for chronic myeloid leukemia. *N Engl J Med*. 2017;376(10):917-927.

4. Daley GQ, Van Etten RA, Baltimore D. Induction of chronic myelogenous leukemia in mice by the P210bcr/abl gene of the Philadelphia chromosome. *Science*. 1990;247(4944):824-830.

5. Morris SW, Kirstein MN, Valentine MB, et al. Fusion of a kinase gene, ALK, to a nucleolar protein gene, NPM, in non-Hodgkin's lymphoma. *Science*. 1994; 263(5151):1281-1284.

6. Stein H, Mason DY, Gerdes J, et al. The expression of the Hodgkin's disease associated antigen Ki-1 in reactive and neoplastic lymphoid tissue: evidence that Reed-Sternberg cells and histiocytic malignancies are derived from activated lymphoid cells. *Blood*. 1985;66(4):848-858.

7. Tsuyama N, Sakamoto K, Sakata S, Dobashi A, Takeuchi K. Anaplastic large cell lymphoma: pathology, genetics, and clinical aspects. *J Clin Exp Hematop*. 2017;57(3):120-142.

8. Fornari A, Piva R, Chiarle R, Novero D, Inghirami G. Anaplastic large cell lymphoma: one or more entities among T-cell lymphoma? *Hematol Oncol*. 2009;27(4):161-170.

9. Savage KJ, Harris NL, Vose JM, et al; International Peripheral T-Cell Lymphoma Project. ALK− anaplastic large-cell lymphoma is clinically and immunophenotypically different from both ALK+ ALCL and peripheral T-cell lymphoma, not otherwise specified: report from the International Peripheral T-Cell Lymphoma Project. *Blood*. 2008;111(12):5496-5504.

10. Kuefer MU, Look AT, Pulford K, et al. Retrovirus-mediated gene transfer of NPM-ALK causes lymphoid malignancy in mice. *Blood*. 1997;90(8): 2901-2910.

11. Turner SD, Tooze R, Maclennan K, Alexander DR. Vav-promoter regulated oncogenic fusion protein NPM-ALK in transgenic mice causes B-cell lymphomas with hyperactive Jun kinase. *Oncogene*. 2003;22(49):7750-7761.

12. Turner SD, Merz H, Yeung D, Alexander DR. CD2 promoter regulated nucleophosmin-anaplastic lymphoma kinase in transgenic mice causes B lymphoid malignancy. *Anticancer Res*. 2006;26:3275-3279.

13. Chiarle R, Gong JZ, Guasparri I, et al. NPM-ALK transgenic mice spontaneously develop T-cell lymphomas and plasma cell tumors. *Blood*. 2003;101(5):1919-1927.

14. Maddalo D, Manchado E, Concepcion CP, et al. In vivo engineering of oncogenic chromosomal rearrangements with the CRISPR/Cas9 system [published correction appears in *Nature*. 2015;524(7566):502]. *Nature*. 2014;516(7531):423-427.

15. van de Krogt J-A, Bempt MV, Ferreiro JF, et al. Anaplastic lymphoma kinase–positive anaplastic large cell lymphoma with the variant RNF213-, ATIC- and TPM3-ALK fusions is characterized by copy number gain of the rearranged ALK gene. *Haematologica*. 2017;102(9):1605-1616.

16. Babin L, Piganeau M, Renouf B, et al. Chromosomal translocation formation is sufficient to produce fusion circular RNAs specific to patient tumor cells. *iScience*. 2018;5:19-29.

17. Cordell JL, Pulford KAF, Bigerna B, et al. Detection of normal and chimeric nucleophosmin in human cells. *Blood*. 1999;93(2):632-642.

18. Grisendi S, Mecucci C, Falini B, Pandolfi PP. Nucleophosmin and cancer. *Nat Rev Cancer*. 2006;6(7):493-505.

19. Pan Z, Hu S, Li M, et al. ALK-positive large B-cell lymphoma: a clinicopathologic study of 26 cases with review of additional 108 cases in the literature. *Am J Surg Pathol*. 2017;41(1):25-38.

20. Beltran B, Castillo J, Salas R, et al. ALK-positive diffuse large B-cell lymphoma: report of four cases and review of the literature. *J Hematol Oncol*. 2009;2(1):11.

21. Krenacs L, Wellmann A, Sorbara L, et al. Cytotoxic cell antigen expression in anaplastic large cell lymphomas of T- and null-cell type and Hodgkin's disease: evidence for distinct cellular origin. *Blood*. 1997;89(3):980-989.

22. Foss HD, Anagnostopoulos I, Araujo I, et al. Anaplastic large-cell lymphomas of T-cell and null-cell phenotype express cytotoxic molecules. *Blood*. 1996; 88(10):4005-4011.

23. Mourali J, Bénard A, Lourenço FC, et al. Anaplastic lymphoma kinase is a dependence receptor whose proapoptotic functions are activated by caspase cleavage. *Mol Cell Biol*. 2006;26(16):6209-6222.

24. Bonvini P, Dalla Rosa H, Vignes N, Rosolen A. Ubiquitination and proteasomal degradation of nucleophosmin-anaplastic lymphoma kinase induced by 17-allylamino-demethoxygeldanamycin: role of the co-chaperone carboxyl heat shock protein 70-interacting protein. *Cancer Res*. 2004;64(9): 3256-3264.

25. Amin AD, Rajan SS, Liang WS, et al. Evidence suggesting that discontinuous dosing of ALK kinase inhibitors may prolong control of ALK+ tumors. *Cancer Res*. 2015;75(14):2916-2927.

26. Robins HS, Campregher PV, Srivastava SK, et al. Comprehensive assessment of T-cell receptor β-chain diversity in alphabeta T cells. *Blood*. 2009; 114(19):4099-4107.

27. Carlson CS, Emerson RO, Sherwood AM, et al. Using synthetic templates to design an unbiased multiplex PCR assay. *Nat Commun*. 2013;4(1):2680.

28. Enomoto T, Lindström MS, Jin A, Ke H, Zhang Y. Essential role of the B23/NPM core domain in regulating ARF binding and B23 stability. *J Biol Chem*. 2006;281(27):18463-18472.

29. Medeiros LJ, Elenitoba-Johnson KSJ. Anaplastic large cell lymphoma. *Am J Clin Pathol*. 2007;127(5):707-722.

30. Piganeau M, Ghezraoui H, De Cian A, et al. Cancer translocations in human cells induced by zinc finger and TALE nucleases. *Genome Res*. 2013;23(7): 1182-1193.

31. Malcolm TIM, Villarese P, Fairbairn CJ, et al. Anaplastic large cell lymphoma arises in thymocytes and requires transient TCR expression for thymic egress. *Nat Commun*. 2016;7(1):10087.

32. Trümper L, Pfreundschuh M, Bonin FV, Daus H. Detection of the t(2;5)-associated NPM/ALK fusion cDNA in peripheral blood cells of healthy individuals. *Br J Haematol*. 1998;103(4):1138-1144.

33. Laurent C, Lopez C, Desjobert C, et al. Circulating t(2;5)-positive cells can be detected in cord blood of healthy newborns. *Leukemia*. 2012;26(1): 188-190.